



# Magnetic nanoparticle ( $\text{Fe}_3\text{O}_4$ ) impregnated onto tea waste for the removal of nickel(II) from aqueous solution

P. Panneerselvam, Norhashimah Morad\*, Kah Aik Tan

Environmental Technology Division, School of Industrial Technology, Universiti Sains Malaysia, 11800 Minden, Penang, Malaysia

## ARTICLE INFO

### Article history:

Received 19 August 2010

Received in revised form 24 October 2010

Accepted 26 October 2010

Available online 2 November 2010

### Keywords:

Magnetic nanoparticle

Tea waste

Isotherm

Kinetics

Thermodynamics

## ABSTRACT

The removal of Ni(II) from aqueous solution by magnetic nanoparticles prepared and impregnated onto tea waste ( $\text{Fe}_3\text{O}_4$ -TW) from agriculture biomass was investigated. Magnetic nanoparticles ( $\text{Fe}_3\text{O}_4$ ) were prepared by chemical precipitation of a  $\text{Fe}^{2+}$  and  $\text{Fe}^{3+}$  salts from aqueous solution by ammonia solution. These magnetic nanoparticles of the adsorbent  $\text{Fe}_3\text{O}_4$  were characterized by surface area (BET), Scanning Electron Microscopy (SEM), Transmission Electron Microscopy (TEM) and Fourier Transform-Infrared Spectroscopy (FT-IR). The effects of various parameters, such as contact time, pH, concentration, adsorbent dosage and temperature were studied. The kinetics followed is first order in nature, and the value of rate constant was found to be  $1.90 \times 10^{-2} \text{ min}^{-1}$  at  $100 \text{ mg L}^{-1}$  and  $303 \text{ K}$ . Removal efficiency decreases from 99 to 87% by increasing the concentration of Ni(II) in solution from 50 to  $100 \text{ mg L}^{-1}$ . It was found that the adsorption of Ni(II) increases by increasing temperature from 303 to 323 K and the process is endothermic in nature. The adsorption isotherm data were fitted to Langmuir and Freundlich equation, and the Langmuir adsorption capacity,  $Q^s$ , was found to be  $(38.3) \text{ mg g}^{-1}$ . The results also revealed that nanoparticle impregnated onto tea waste from agriculture biomass, can be an attractive option for metal removal from industrial effluent.

© 2010 Elsevier B.V. All rights reserved.

## 1. Introduction

In recent years, magnetic nanoparticles have attracted much attention because of their unique magnetic properties and widespread application in different fields such as mineral separation, magnetic storage devices, catalysis, magnetic refrigeration system, heat transfer application in drug delivery system, magnetic resonance imaging (MRI), cancer therapy, and magnetic cell separation [1–7]. The application of magnetite in the field of waste water treatment is becoming an interesting area of research. Nanoparticle exhibit good adsorption efficiency especially due to higher surface area and greater active sites for interaction with metallic species and can easily be synthesized; several researches have used it as an adsorbent [8–12]. Nickel is the 24th element in order of natural abundance in earth crust [13]. Nickel is a common metal and it is frequently used in different industries, viz., electroplating, dyeing, storage batteries, porcelain enameling, pigment and steel manufacturing, etc. [14,15]. The tolerance limit of nickel in drinking water is  $0.01 \text{ mg L}^{-1}$ , and for industrial wastewater it is  $2.0 \text{ mg L}^{-1}$  [16]. However, effluents of different industries contain higher concentration of nickel than its acceptable limit. Although nickel is an essential micronutrient for animals and takes part in synthesis

of vitamin  $\text{B}_{12}$ , its higher concentration cause cancer of the lungs, nose, and bones and it may also cause nausea, rapid respiration, headache, cyanosis, and dry cough [17,18]. It is thus necessary to treat industrial effluent rich in Ni(II) before their discharge.

Many technologies such as ion exchange, reduction flocculation, membrane filtration, precipitation, electrochemical, filtration and reverse osmosis have been proposed by different scientific workers for the removal of nickel from aqueous solution and effluents. However, most of these technologies require high operational and maintenance costs, and also generate toxic sludge [19,20]. Due to high expense, these techniques are not suitable for small scale industries especially in developing country. Adsorption is one of the most promising techniques for the removal of metallic pollutants from industrial effluents [21]. Adsorption offers high efficiency, cost effectiveness, and easy handling among the majority of physiochemical treatment methods. Among the waste treatment procedures, adsorption techniques are the most widely used as low-cost alternative technology. Cheaper and effective adsorbents can be formed from abundant natural materials or certain waste materials (or products) from industrial and agricultural activities. In general, an adsorbent which requires little processing or is abundant in nature or is a by-product or waste material from another industry is called a “low-cost” adsorbent [22]. In recent years, a vast number of publications have been dedicated to the removal of heavy metals from wastewater by using adsorption techniques with different low-cost materials, such as moss peat [23], coconut

\* Corresponding author. Tel.: +60 46532236; fax: +60 46573678.  
E-mail address: [nhashima@usm.my](mailto:nhashima@usm.my) (N. Morad).

husk, a sugar industry waste [24], chitin [25], sawdust [26,27], green algae [28,29], fly ash [30], bone char [31], lignite [32], zeolite [33–35], wood [36], tea waste [37–40], etc.

The aim of the present research is to explore the feasibility of utilizing tea waste as a single use and low-cost filter for metal removal in industrial wastewater. Insoluble cell walls of tea leaves are largely made up cellulose and hemicelluloses, lignin, condensed tannins and structural proteins. In other words, one third of the total dry matter in tea leaves should have good potential as metal scavengers from solutions and wastewaters since the above constituents contain functional groups. The responsible groups in lignin, tannin or other phenolic compounds are mainly carboxylate, aromatic carboxylate, phenolic hydroxyl and oxyl groups [41,42]. The poly structure of cellulose-based materials has relatively strong chemical adsorption cations such as metal ions and organic bases as well as physical adsorption to other materials such as acidic and anionic compounds [43].

The present study is undertaken for the better application and management of such a valuable agricultural biomass for useful purpose. Although there are many researches concentrating on adsorptive materials from agricultural waste, research on modification of these wastes using magnetic nanoparticles have not been reported before. This paper reports the preparation of magnetic nanoparticles impregnated onto tea waste as low-cost active adsorbent and its effectiveness in removing nickel ions from aqueous solution at various conditions.

## 2. Materials and methods

### 2.1. Chemicals

All chemicals used were of analytical grade and supplied by Sigma–Aldrich (M) Sdn Bhd, Malaysia. The chemicals used in this study were nickel sulfate, ferrous chloride, ferric chloride, ammonia solution, acetone, hydrochloric acid, sodium hydroxide, ethyl alcohol, and dimethyl glyoxime.

### 2.2. Adsorbent

Waste tea leaves produced from domestic tea making process were used for making adsorbent. The tea dust discarded after being used is called tea waste. The collected materials were then washed with distilled water for several times to remove all the dirt particles. It was then boiled with distilled water at 80 °C for 1 h to remove caffeine, tannin and color, and then washed with distilled water until the washing water contains no color. The color of the solution was spectrometrically observed at room temperature. Decolorized and cleaned tea waste was dried in an oven at 105 °C for 10 h. The dried materials were then crushed and sieved (100 μm) and stored in a bottle.

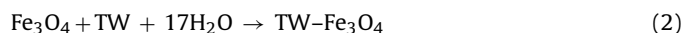
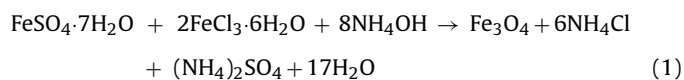
### 2.3. Preparation of Fe<sub>3</sub>O<sub>4</sub>-TW

The chemical precipitation technique has been used to prepare particles with homogeneous composition and narrow size distribution [44]. This technique is probably the most common and efficient method to obtain magnetic particles. A complete precipitation of Fe<sub>3</sub>O<sub>4</sub> was achieved under alkaline condition, while maintaining a molar ratio of Fe<sup>2+</sup> to Fe<sup>3+</sup>, 1:2, under inert environment. To obtain 2 g of magnetic particles, 2.1 g of FeSO<sub>4</sub>·7H<sub>2</sub>O and 3.1 g of FeCl<sub>3</sub>·6H<sub>2</sub>O were dissolved under inert atmosphere in 80 mL of double distilled water with vigorous stirring. While the solution was heated to 80 °C, 10 mL of ammonium hydroxide solution (25%) was added. To ensure complete growth of the nanoparticle crystals, the solution was then added to 10 g of tea waste and reaction was



Fig. 1. Photographic picture of Fe<sub>3</sub>O<sub>4</sub> onto magnetic rod.

carried out for 30 min at 80 °C under constant stirring. The resulting suspension was cooled down to room temperature and then repeatedly washed with double distilled water to remove unreacted chemicals. Fe<sub>3</sub>O<sub>4</sub>-TW adsorbent were tested with magnetic rod as shown in Fig. 1, and it is clearly observed that all the iron oxide were attracted to the magnetic rod, because of the magnetic behavior of the iron. The reactions that occur in the production of magnetic nanoparticles (Fe<sub>3</sub>O<sub>4</sub>-TW) are as shown in Eqs. (1) and (2).



### 2.4. Adsorbent analysis methods

The magnetic nanoparticles (Fe<sub>3</sub>O<sub>4</sub>-TW) were characterized by BET, SEM, TEM and FT-IR. The BET (Brunauer, Emmett and Teller) surface areas of the adsorbent materials were measured using Smart Sorbs 92 surface area analyzer where N<sub>2</sub> gas was used as adsorbate. The SEM (Scanning Electron Microscopy) measurements were carried out using SEM-Quanta. The images were taken with an emission current = 100 μA by the Tungsten filament and an accelerator voltage = 10 kV. The morphology and dimensions of the adsorbent were determined by TEM (Transmission Electron Microscopy) (JEOL-2010). Fourier transform infrared spectroscopy of the adsorbent was done by using an FT-IR spectrophotometer (Model: FT-IR Bruker IFS 66 V). Spectra obtained in the range of 500–4000 cm<sup>-1</sup> were analyzed.

### 2.5. Adsorption studies

Batch adsorption studies were conducted to determine equilibrium time. A stock solution of Ni(II) was prepared by dissolving 4.479 g of NiSO<sub>4</sub>·6H<sub>2</sub>O in 1000 mL of distilled water. Batch adsorption studies were performed by mixing 0.25 g magnetic nanoparticle impregnated with tea waste (Fe<sub>3</sub>O<sub>4</sub>-TW) with 50 mL of Ni(II) solution of varying concentration in 250 mL conical flask. The dosage of adsorbent was decided by the requirements of the experiments. The pH of the solution was adjusted by adding diluted HCl and NaOH. All the adsorption experiments were conducted at temperature 303 K, at the pH working solution, vis., 4, and at an agitation rate at constant speed of 100 rpm. After equilibrium, the sample was centrifuged and the filtrates were analyzed by a

UV-visible spectrophotometer at 445 nm using the dimethyl glyoxime (DMG) method [45]. The percentage removal of Ni(II) was calculated by the following equation.

$$\text{Percentage removal of Ni(II) ions} = \frac{C_0 - C_e}{C_0} \times 100 \quad (3)$$

$$\text{Amount adsorbed in Ni(II) ions } (q_e) = \frac{(C_0 - C_e)V}{m} \quad (4)$$

where  $C_0$  and  $C_e$  are the initial and equilibrium concentration of Ni(II) ( $\text{mg L}^{-1}$ ) respectively,  $m$  is the mass of the adsorbent (g) and  $V$  is the volume of Ni(II) solution (L).

### 2.6. Studies on Point zero charge ( $\text{PH}_{\text{zpc}}$ )

In  $\text{PH}_{\text{zpc}}$  determination, 0.01 M NaCl was prepared and its pH was adjusted in the range of 2–12 by adding NaOH or HCl. Then, 50 mL of 0.01 M NaCl each was put in three different conical flasks and then 0.25 g of the three adsorbents were added to these solutions [4]. These flasks were kept for 48 h and final pH of the solution was measured by using pH meter. Graphs were then plotted for  $\text{pH}_{\text{final}}$  versus  $\text{pH}_{\text{initial}}$ .

## 3. Results and discussion

### 3.1. BET, SEM and TEM analysis

The BET surface areas of both unmodified tea waste (also known as parent TW) and the modified tea waste samples were deter-

mined. It was found that the surface areas of parent tea waste (TW) and magnetic nanoparticle impregnated tea waste ( $\text{Fe}_3\text{O}_4\text{-TW}$ ) were 22.3 and 27.5  $\text{m}^2 \text{g}^{-1}$  respectively. In order to observe the surface of particles before and after modification of TW, SEM images for the samples of the parent tea waste (TW), magnetic nanoparticle impregnated to TW ( $\text{Fe}_3\text{O}_4\text{-TW}$ ) and after metal ions adsorption with TW are shown in Fig. 2a to d. The TW materials have insoluble cell walls with fibrous content and are largely made up of cellulose-based structural proteins. A high response surface of the functional groups is also present. As shown in Fig. 2a, the parent TW material has more fiber and more active sites, and the active sites can be clearly observed at 100  $\mu\text{m}$ . Fig. 2b shows the parent tea waste is completely covered with iron oxide, and all the iron oxide particles are aggregated to form a spherical and cage-like structure. Fig. 2c shows a single TW fibrous material with more holes and active sites available at 30  $\mu\text{m}$  since the iron oxide are occupying the active sites. Fig. 2d shows the SEM image, after adsorption of the Ni(II) metal ions onto  $\text{Fe}_3\text{O}_4\text{-TW}$ . Compared to Fig. 2b, more particles are present on the surface of the  $\text{Fe}_3\text{O}_4\text{-TW}$ . These particles are the Ni(II) ions as well as the iron oxide particles. The iron oxide particles exhibit magnetic behavior, creating more negative charges. The positively charge Ni(II) ions will be electrostatically attracted to the adsorbent. This is depicted by more particles being adsorbed as shown in Fig. 2d.

TEM images with surface morphology of the particles and three different adsorbents, i.e., TW-Ni(II),  $\text{Fe}_3\text{O}_4\text{-Ni(II)}$  and  $\text{Fe}_3\text{O}_4\text{-TW-Ni(II)}$  are shown in Fig. 3a–c respectively. Fig. 3a shows the parent TW adsorbed with Ni(II) ions at 100 nm. As evident in the figure,

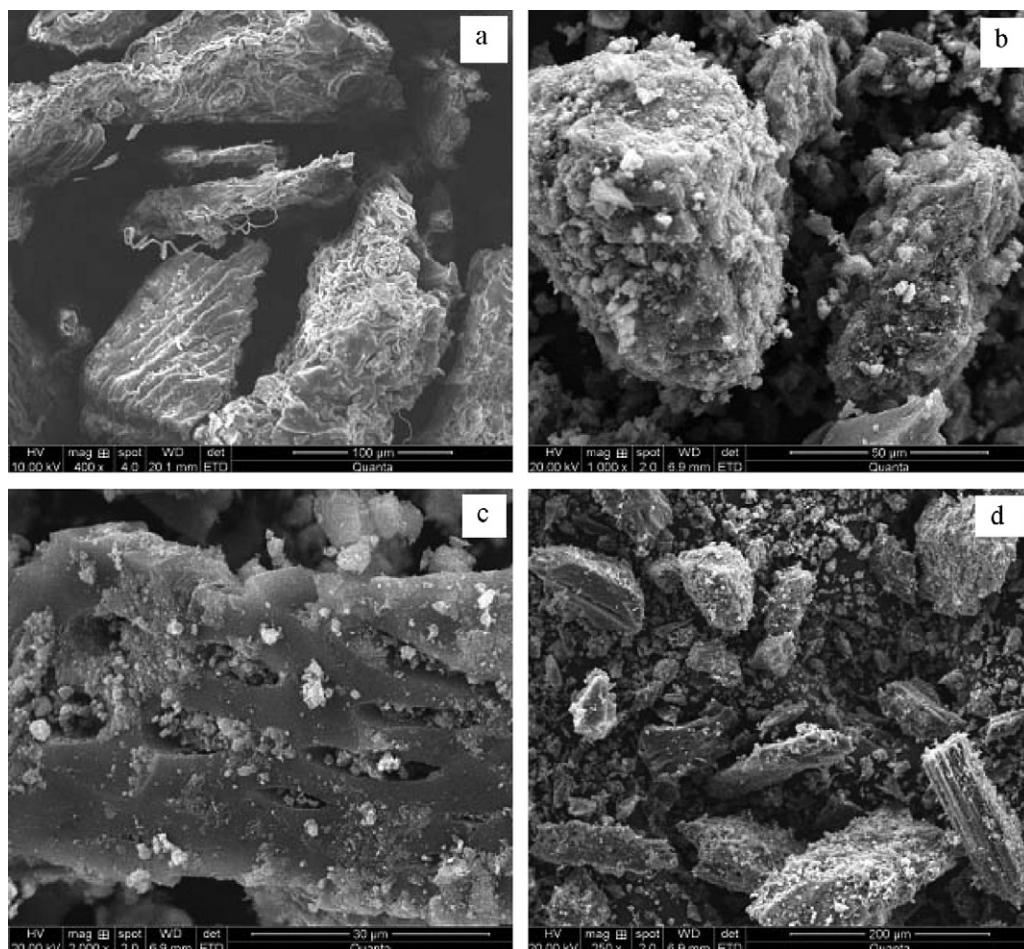


Fig. 2. SEM image of (a) Parent TW, (b) and (c)  $\text{Fe}_3\text{O}_4\text{-TW}$ , (d) Ni(II)- $\text{Fe}_3\text{O}_4\text{-TW}$ .

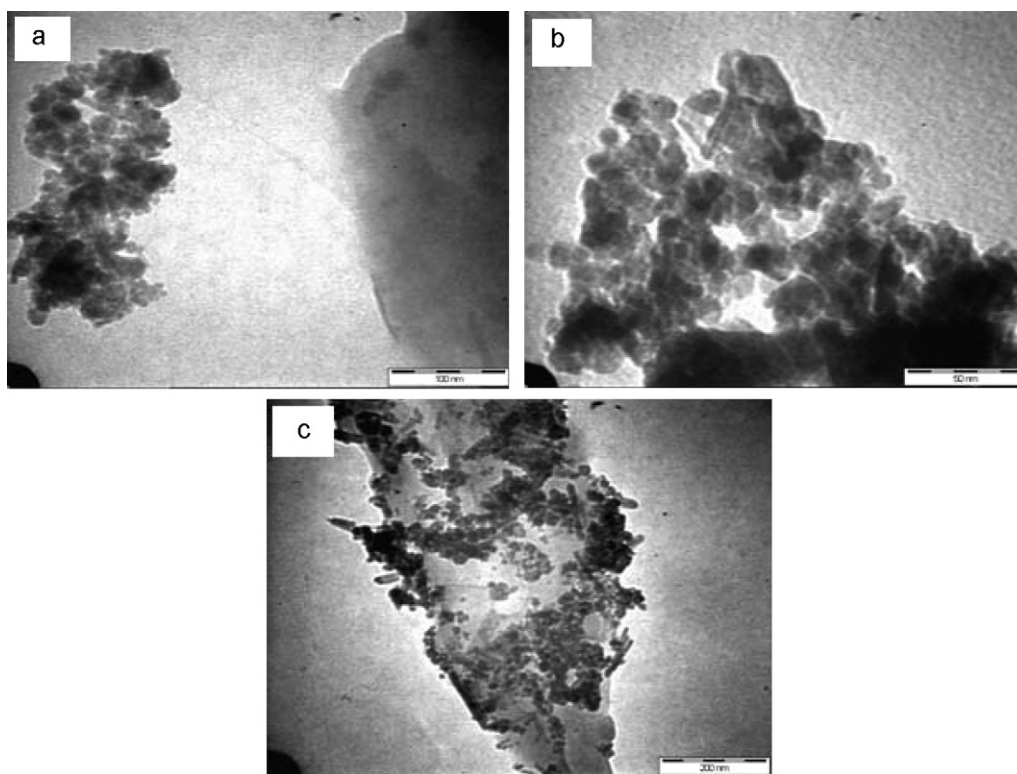


Fig. 3. TEM image of (a) Parent TW–Ni(II), (b) Fe<sub>3</sub>O<sub>4</sub>–Ni(II) and (c) Fe<sub>3</sub>O<sub>4</sub>–TW–Ni(II).

the Ni(II) ion particles aggregated to the surface of the TW and bind in the form of clusters. Fig. 3b shows the Ni(II) ions particle with spherical shape, aggregating onto iron oxide surface. In Fig. 3c, the Ni(II) ions are adsorbed onto Fe<sub>3</sub>O<sub>4</sub>–TW. It is observed that more Ni(II) ions particles are occupying the adsorbent, compared to the Fe<sub>3</sub>O<sub>4</sub> and TW adsorbents. Therefore, the Ni(II) ion is removed more efficiently by the Fe<sub>3</sub>O<sub>4</sub>–TW adsorbent.

### 3.2. Fourier transforms infrared spectroscopy analysis

The FT-IR spectra of both modified and unmodified tea waste are shown in Fig. 4a and b, and the FT-IR spectroscopic characteristics are shown in Table 1. The functional groups of tea waste and the corresponding infrared absorption frequency are shown in Table 1 and Fig. 4, respectively. The spectra display a number of absorption peaks, indicating the complex nature of tea waste. The troughs, due to bonded OH groups, are observed in the range of 3340–3380 cm<sup>-1</sup> [45]. The FT-IR spectroscopic analysis indicated broad bands at 3420 cm<sup>-1</sup>, representing bonded –OH groups. The band observed at about 2920–2850 cm<sup>-1</sup> could be assigned to the aliphatic C–H group [46,47]. At wave number 1733 cm<sup>-1</sup> a

shoulder is observed which may be due to the carbonyl stretch of carboxyl. The trough at 1640–1660 cm<sup>-1</sup> represents the C=O stretching mode conjugate with the NH<sub>2</sub> (amide 1 band) [46]. In some studies, this spectrum represents a cleared form of the carbonyl on the carboxyl group [47]. In other studies this peak was described as the region of both ionized–noncoordinated and ionized coordinated COO<sup>-</sup> group [48,49]. The peak observed at 1543 and 1520 cm<sup>-1</sup> corresponds to the secondary amine group. Symmetric bending of CH<sub>3</sub> is observed to shift to 1456 cm<sup>-1</sup> [40]. The peak observed at 1240 and 1143 cm<sup>-1</sup> could be assigned to –SO<sub>3</sub> stretching and C–O stretching of ether groups, respectively [40].

When comparing the two spectra in Fig. 4a and b, Fig. 4b shows that there were various functional groups detected on the surface of Fe<sub>3</sub>O<sub>4</sub>–TW and a small peak is observed in the Fe–O group. There are some peaks that were shifted, disappeared and new peaks were produced. Significant band decrease of functional group on the Fe<sub>3</sub>O<sub>4</sub>–TW were detected at bands 1732, 1445 and 1155, which corresponded to the bonded C=O stretching, aromatic nitro compound and –C–C– groups respectively. The newer peak at 661 cm<sup>-1</sup> observed in Fig. 4b is related to the Fe–O group, and the peak around 3420 cm<sup>-1</sup> in curve a was assigned to the –OH group on the surface of the magnetite. These two significant bands in the spectrum indicate the possible involvement of those functional groups on the surface of Fe<sub>3</sub>O<sub>4</sub>–TW process. Thus, it seems that this type of functional group is likely to participate in metal binding. Fig. 4c shows the FTIR spectrum after adsorption of Ni(II) ions onto Fe<sub>3</sub>O<sub>4</sub>–TW. When comparing the two spectra of Fig. 4b and c, Fig. 4c shows that the hydroxyl group are present in the range of peak at 3340 cm<sup>-1</sup>. This peak has shifted and changes the region of the peaks, because the hydroxyl groups are likely to participate in the Ni(II) ion adsorption. A well-known mechanism involved in the adsorbate and adsorbent interaction is governed by ion exchange process and followed by the adsorption process. In the adsorption process, H<sup>+</sup> ions leaving groups of the adsorbent bound with Ni(II) ions at the adsorbent surface due to electrostatic attraction.

**Table 1**  
The FT-IR spectral characteristic of Fe<sub>3</sub>O<sub>4</sub>–TW.

IR peak	Frequencies (cm <sup>-1</sup> )	Assignment
1	3342	Boded –OH groups
2	2924	Aliphatic C–H groups
3	2856	Aliphatic C–H groups
4	1732	C=O stretching
5	1648	Symmetric bending of CH <sub>3</sub>
6	1445	Symmetric bending of CH <sub>3</sub>
7	1240	–SO <sub>3</sub> stretching
8	1155	C–O stretching of ether groups
9	1033	–C–C– group
10	614	–CN– stretching

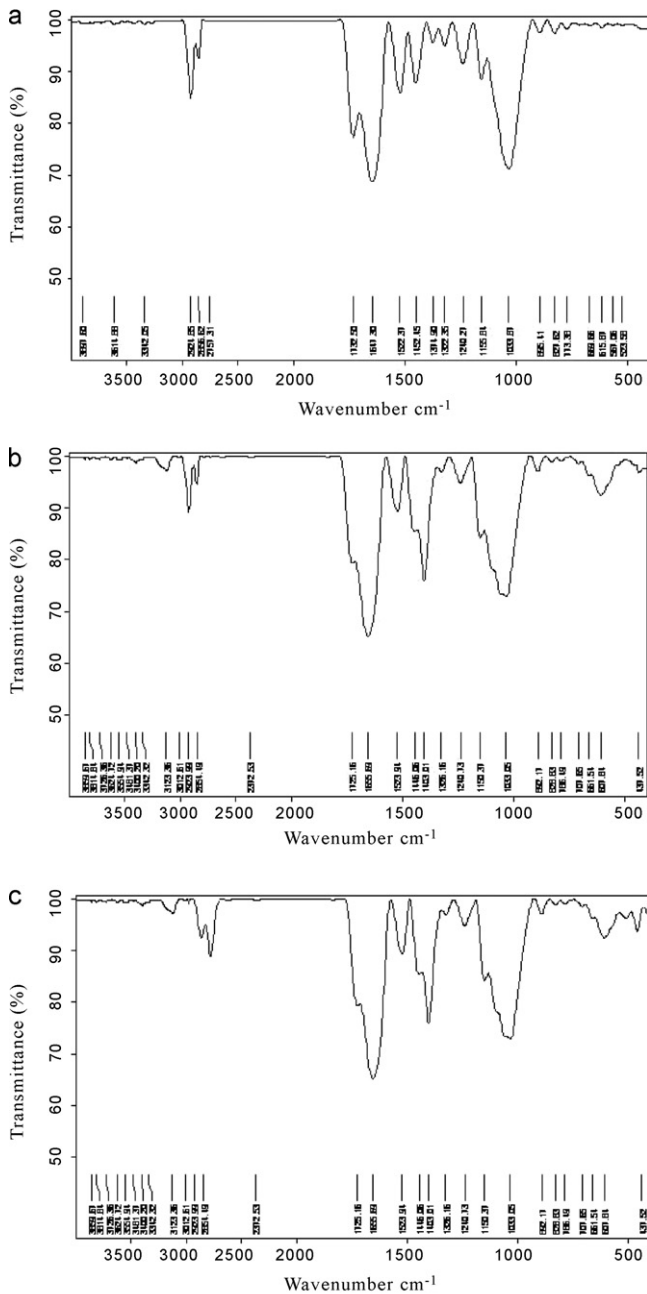


Fig. 4. FT-IR spectra of (a) parent tea waste and (b)  $\text{Fe}_3\text{O}_4$ -TW.

### 3.3. Determination of point zero charge ( $\text{pH}_{\text{zpc}}$ )

Point zero charges ( $\text{pH}_{\text{zpc}}$ ) were determined for three adsorbent, i.e., TW,  $\text{Fe}_3\text{O}_4$  and  $\text{Fe}_3\text{O}_4$ -TW.  $\text{pH}_{\text{zpc}}$  is an important property and indicates the electrical neutrality of the adsorbent and surface at a particular value of pH. The graph of  $\text{pH}_{\text{initial}}$  and vs  $\text{pH}_{\text{final}}$  was plotted as shown in Fig. 5. The intersections of the curves with the straight line are known as the end points of the  $\text{pH}_{\text{zpc}}$ , and these values are 5.8, 6.2 and 6.5 for TW,  $\text{Fe}_3\text{O}_4$  and  $\text{Fe}_3\text{O}_4$ -TW respectively.

### 3.4. Effect of contact time and initial concentration

Two parameters, namely, contact time and initial concentration, have a pronounced effect on the removal of adsorbate species from aqueous solution. In the present study, the effect of initial concentration of Ni(II) on its removal from aqueous solutions

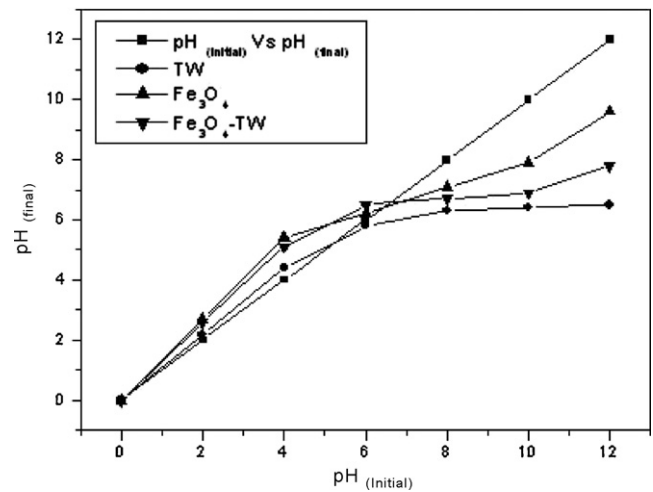


Fig. 5. Plot for determination of point zero charge of TW,  $\text{Fe}_3\text{O}_4$  and  $\text{Fe}_3\text{O}_4$ -TW.

was carried out. The removal efficiency increased from 90 to 96% with the increase of initial concentrations of Ni(II) from 50 to  $100 \text{ mg L}^{-1}$ , with adsorbent dose of 0.25 g, temperature 303 K for 3 h, and shaking speed of 100 rpm, at best removal condition as shown in Fig. 6. It is clear from Fig. 6 that the graphs are single and smooth, indicating monolayer coverage of the adsorbent surface by Ni(II). In addition, the removal is rapid in the initial stages, saturates slowly, and acquires a maximum removal at the time of equilibrium, viz., 120 min.

### 3.5. Effect of adsorbent dosage

Adsorbent dose is an important parameter in the determination of adsorption capacity. As the adsorbent dosage increases, the adsorbent sites available for Ni(II) metal ions are also increased and consequently better adsorption takes place. In the present study, the adsorbent dosages were varied from 0.40 to 0.60 g in 50 mL and  $100 \text{ mg L}^{-1}$  Ni(II) solutions, while all the other variables such as rpm, contact time and temperature were kept constant. This method is also known as optimization based on one factor at a time where one parameter is varied, and the others are kept constant [3,4]. The results are shown in Fig. 7. The trend of the graph shows that as the contact time increases, the percentage removal also increase, until it reaches a saturation point, where the increase in contact time does not change the percentage removal. The best

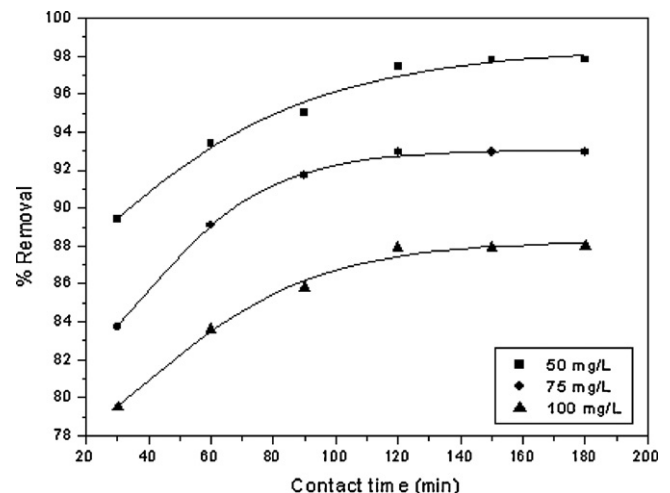


Fig. 6. Effect of initial concentration on percent removal of Ni(II).

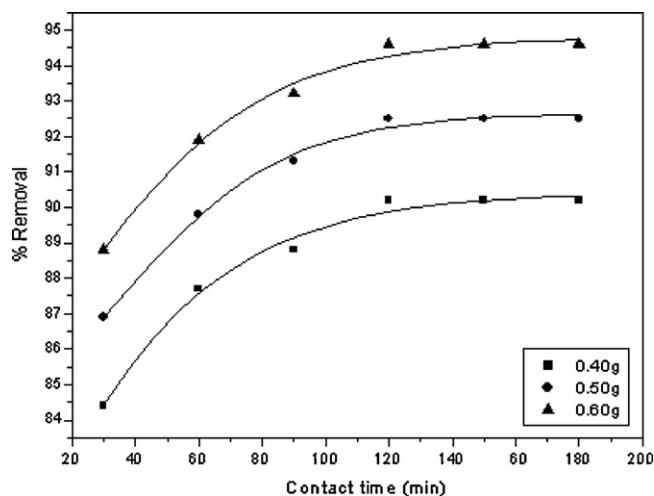


Fig. 7. Effect of adsorbent dose on percent removal Ni(II).

removal of Ni(II) is at about 94%, using an adsorbent dosage of 0.60 g in 100 mg L<sup>-1</sup> Ni(II) solution.

### 3.6. Effect of pH

The effect of pH of the suspending medium on nickel removal was studied by performing equilibrium adsorption experiments at different pH values. The results are illustrated in Fig. 8. The effect of pH on Ni(II) adsorption is examined in the pH range 2–7. All the variables such as, dosage, rpm, contact time and temperature were kept constant. For the magnetic nanoparticle impregnated with tea waste (Fe<sub>3</sub>O<sub>4</sub>-TW) the uptake efficiency gradually increases as the pH increases from 2 to 4. At lower pH, the concentration of H<sup>+</sup> ion is high, causing a competition for vacant adsorbent site between the H<sup>+</sup> ion and Ni(II) cations. Therefore, at low pH, the removal efficiency is low. After pH 4, the adsorption capacity remains constant and uptake of Ni(II) ions is observed which could be attributed to precipitation of Ni(II) as Ni(OH)<sub>2</sub>. Hence the optimum pH range for the removal of Ni(II) was found to be 4.

### 3.7. Kinetic studies

The kinetic study of adsorption processes provides useful data regarding the efficiency of the adsorption and the feasibility for

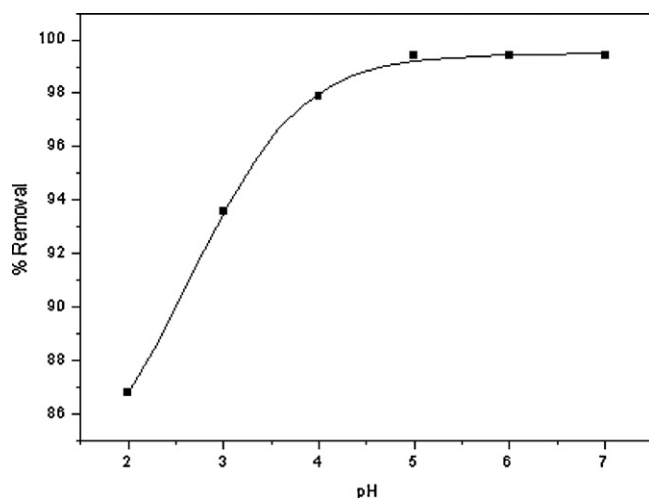


Fig. 8. Effect of pH on percent removal Ni(II).

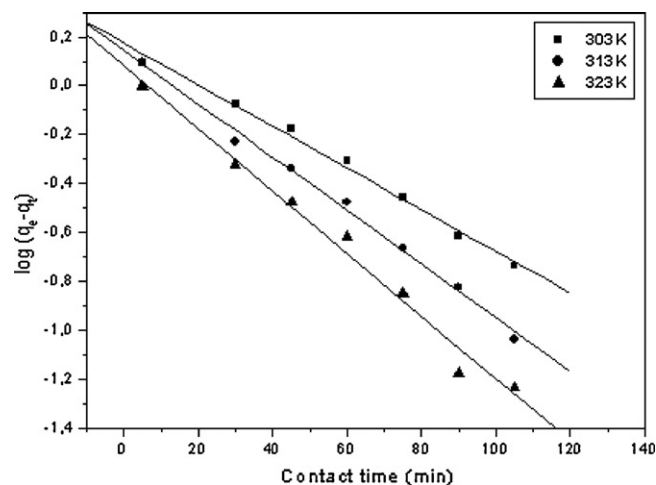


Fig. 9. Lagergrens plot for kinetic modeling of the adsorption process of Ni(II) on Fe<sub>3</sub>O<sub>4</sub>-TW.

scale-up operations. The kinetic data of adsorption can be evaluated using different types of mathematic models, of which one most widely used is Lagergren's rate equation [50,51]. The kinetic of the adsorption process was analyzed using the first-order rate equation given by

$$\frac{dq_t}{dt} = k_1(q_e - q_t) \quad (5)$$

On integration with limits from  $t=0$  to  $t$  and  $q_1=0$  to  $q_1$ ,

$$\log(q_e - q_t) = \log q_e - \frac{k_1}{2.303} t \quad (6)$$

where  $q_e$  and  $q_t$  are the concentration of the Ni(II) ions (mg g<sup>-1</sup>) at equilibrium and time  $t$ , respectively, after the adsorption processes  $k_1$  is the adsorption rate constant for the Ni(II) adsorption. The straight line plots of  $\log(q_e - q_t)$  vs  $t$ , shown in Fig. 9, confirm that the process of removal is governed by first-order kinetics. The linear plots also demonstrated the applicability of Lagergren's model for this study. The value of  $k_1$  was determined by the slope of the plot and was found to be  $1.90 \times 10^{-2} \text{ min}^{-1}$  at 100 mg L<sup>-1</sup> concentration and 303 K. The values of  $k_1$ , shown in Table 2, indicate that magnetic nanoparticle impregnated onto tea waste (Fe<sub>3</sub>O<sub>4</sub>-TW) can be used for the Ni(II) removal from aqueous solution.

### 3.8. Equilibrium modeling

Equilibrium modeling of the process of removal of nickel was carried out by using the Langmuir and Freundlich adsorption isotherm [52,53]. Several mathematical models have been applied in describing equilibrium studies for the removal of pollutants by adsorption on solid surface. Selection of an isotherm equation depends on the nature and type of the system. Out of several isotherm equations, the Freundlich and Langmuir isotherm equation have been reported most frequently. The Langmuir model assumes that uptake of metal ions occurs on a homogeneous surface by monolayer adsorption and that there is no interaction between sorbed species. The Langmuir equation is expressed by the follow-

Table 2  
Values of rate constant of adsorption.

Temp (K)	$k_1 (\times 10^{-2} \text{ min}^{-1})$	$q_e (\text{mg g}^{-1})$	$R^2$
303	1.9	1.491	0.991
313	2.5	1.538	0.994
323	3.8	1.653	0.993

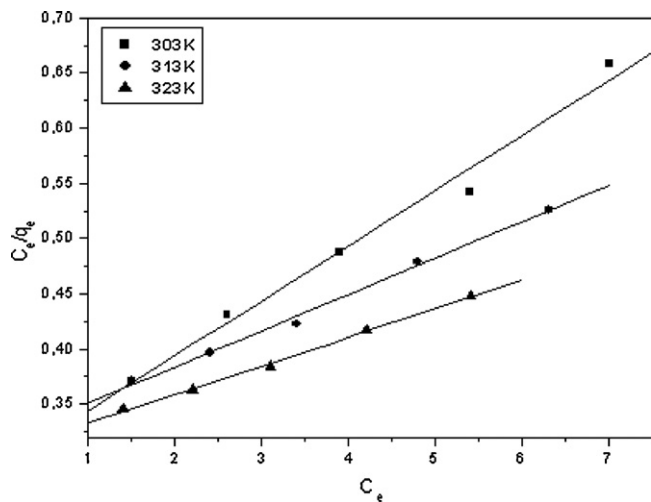


Fig. 10. Langmuir isotherm plot for the removal of Ni(II) on Fe<sub>3</sub>O<sub>4</sub>-TW.

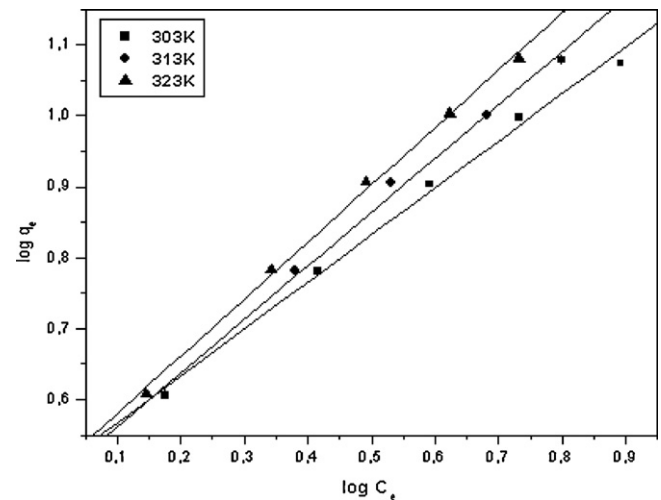


Fig. 11. Freundlich isotherm plot for the removal of Ni(II) on Fe<sub>3</sub>O<sub>4</sub>-TW.

ing expression:

$$\frac{C_e}{q_e} = \frac{1}{Q^{\circ}b} + \frac{C_e}{Q^{\circ}} \quad (7)$$

where  $C_e$  is the equilibrium concentration of the solute ( $\text{mg L}^{-1}$ ),  $q_e$  is the amount adsorbed at equilibrium ( $\text{mg g}^{-1}$ ), and  $Q^{\circ}$  ( $\text{mg g}^{-1}$ ) and  $b$  ( $\text{L mg}^{-1}$ ) are constants related to the adsorption capacity and energy of adsorption, respectively. A plot of  $C_e/q_e$  versus  $C_e$  as shown in Fig. 10, gives a straight line. The value of  $Q^{\circ}$  and  $b$  were determined by the slopes and intercept of Fig. 10, and are given in Table 3.

The Freundlich model assumes that the uptake of metal ions occurs on a heterogeneous adsorbent surface. The Freundlich equation is expressed as:

$$q_e = K_F C_e^{1/n} \quad (8)$$

$$\log q_e = \log K_F + \frac{1}{n} \log C_e \quad (9)$$

where  $K_F$  and  $1/n$  are related the adsorbent capacity and sorption intensity of the adsorbent, respectively. The values of Freundlich constants,  $K_F$  and  $1/n$ , were determined by slopes and intercept of Fig. 11. The high  $R^2$  values obtained as shown in Table 3, indicate that experimental data obeyed both Langmuir and Freundlich isotherm models. Table 4, shows the adsorption capacities of various adsorbents. It is clear from this table that the adsorption capacity of magnetic nanoparticle impregnated to tea waste (Fe<sub>3</sub>O<sub>4</sub>-TW) used in the present studies is significant. The manufacture of this adsorbent could be upscaled and produced in small-scale industries. Tea waste could be utilized to make value added product, i.e., adsorbent, which could be used to treat wastewater [37–40].

### 3.9. Effect of different adsorbent (Fe<sub>3</sub>O<sub>4</sub>-TW) ratio

The effect of three different adsorbent, i.e., TW, Fe<sub>3</sub>O<sub>4</sub> and Fe<sub>3</sub>O<sub>4</sub>-TW on the percentage removal Ni(II) ion were investi-

**Table 4**  
Comparison of adsorption capacities  $Q^{\circ}$  ( $\text{mg g}^{-1}$ ) of different adsorbents for the removal of Ni(II).

Adsorbents	Adsorption capacity	Reference
Bagasse	0.001	[24]
Fly ash	0.03	[24]
Aspergillus niger	1.10	[46]
Granular activated carbon	1.50	[16]
Rice hull	5.75	[59]
Sheep manure waste	7.20	[54]
Deactivated protanated yeast	9.01	[58]
Peat moss	9.18	[23]
Coir pith	9.50	[14]
Calcium alginate	10.50	[55]
Sugar beet pulp	10.74	[57]
Beaker yeast	11.40	[8]
Fe <sub>3</sub> O <sub>4</sub>	11.53	[3]
Thuja orientalis	12.42	[18]
Carbon aerogel	12.87	[56]
Waste tea	18.42	[38]
Fe <sub>3</sub> O <sub>4</sub> -TW	38.30	Present study

gated. The settings of the parameters were based on optimized parameters of initial concentration  $100 \text{ mg L}^{-1}$ , adsorbent dosage of  $0.25 \text{ g}$ , temperature  $303 \text{ K}$  for  $3 \text{ h}$ , and shaking speed of  $100 \text{ rpm}$ . The percentage removal obtained are Fe<sub>3</sub>O<sub>4</sub>-TW (Ratio TW:Fe<sub>3</sub>O<sub>4</sub>; 5:1) 87%, Fe<sub>3</sub>O<sub>4</sub> 46.5% and TW 29.8% respectively. The percentage removal is as shown in Fig. 12 (a). The percentage removal of Ni(II) ions using different adsorbent ratios (TW: Fe<sub>3</sub>O<sub>4</sub>) such as 5:1, 5:2, 5:3, 5:4 and 5:5 are as shown in Fig. 12(b). As illustrated in the figures, the percentage removal increases with increasing iron oxide ratio, but the removal remained almost constant after 5:2. This ratio is suitable to be used in the removal of metal ions since the surface area of TW is completely occupied by iron oxide.

**Table 3**  
Values of Langmuir and Freundlich constants for the removal of Ni(II).

Langmuir constants	Freundlich constants						
	Temp (K)	$Q^{\circ}$ ( $\text{mg g}^{-1}$ )	$b$ ( $\text{L g}^{-1}$ )	$R_L^2$	$n$	$K_F$ ( $\text{L g}^{-1}$ )	$R_F^2$
	303	22.4	0.144	0.997	1.23	3.15	0.989
	313	30.9	0.103	0.994	1.50	3.17	0.970
	323	38.3	0.085	0.996	1.78	4.85	0.975

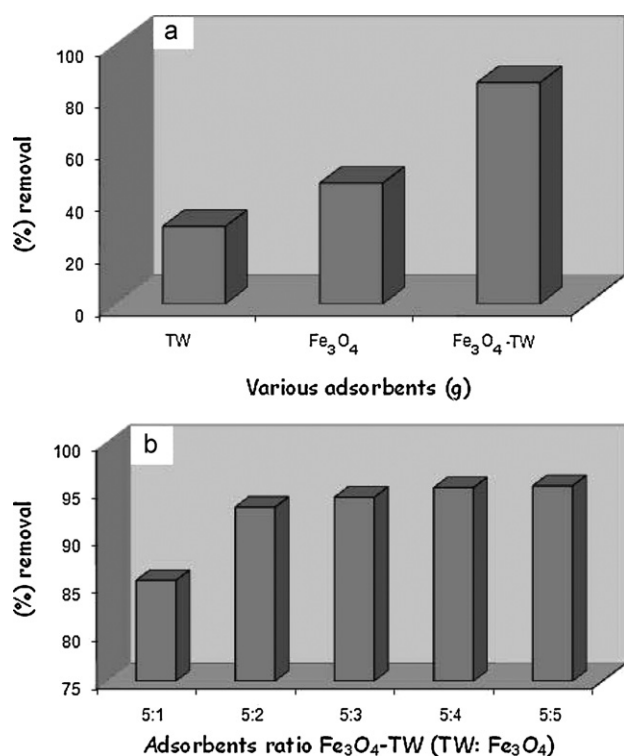


Fig. 12. Percentage removal of Ni(II) ions onto (a) TW, Fe<sub>3</sub>O<sub>4</sub> and Fe<sub>3</sub>O<sub>4</sub>-TW (b). Different ratio of TW and Fe<sub>3</sub>O<sub>4</sub>.

### 3.10. Thermodynamic studies

Thermodynamic studies are used to decipher any reaction in a better way. In the present studies also, thermodynamic studies were performed and the parameters, namely, free energy change ( $\Delta G^\circ$ ), enthalpy ( $\Delta H^\circ$ ), and entropy ( $\Delta S^\circ$ ), were determined at 303, 313 and 323 K, respectively. Thermodynamic parameter were calculated by using the following equations [4]:

$$K_c = \frac{C_{ac}}{C_e} \quad (10)$$

$$\Delta G^\circ = -RT \ln K_c \quad (11)$$

$$\Delta H^\circ = R \frac{T_2 T_1}{T_2 - T_1} \ln \frac{K_2}{K_1} \quad (12)$$

$$\Delta S^\circ = \frac{\Delta H^\circ - \Delta G^\circ}{T} \quad (13)$$

$K_c$  is the equilibrium constant and  $C_{ac}$  and  $C_e$  are the equilibrium concentration of metal ions on the adsorbent ( $\text{mg L}^{-1}$ ) and the equilibrium concentration of the metal ions in the solution ( $\text{mg L}^{-1}$ ), respectively. The values of  $K_c$  increased as the temperature is increased, indicating the endothermic nature of the process of removal. The values of these parameters are given in Table 5. Positive value of entropy change  $\Delta S^\circ$  and enthalpy change  $\Delta H^\circ$  also indicate the endothermic nature of adsorption of Ni(II) in magnetic nanoparticle impregnated onto tea waste (Fe<sub>3</sub>O<sub>4</sub>-TW). It is noted that values of  $\Delta G^\circ$  decreases by increasing temperature.

Table 5  
Thermodynamic parameters for adsorption of Ni(II).

Temp (K)	$-\Delta G^\circ$ (kcal mol <sup>-1</sup> )	$\Delta H^\circ$ (kcal mol <sup>-1</sup> )	$\Delta S^\circ$ (kcal mol <sup>-1</sup> )
303	7.23		
313	8.31	33.41	0.5797
323	10.02		

This reveals that a greater adsorption can be obtained at higher temperature.

## 4. Conclusions

The efficiency of magnetic nanoparticle impregnated onto tea waste (Fe<sub>3</sub>O<sub>4</sub>-TW) in removing nickel(II) ions from aqueous solution has been investigated. Results indicate that adsorption is positively dependent on pH and temperature. A higher percentage removal of nickel could be obtained at lower initial nickel concentration. The adsorption data were well fitted by both the Langmuir and Freundlich isotherm. The adsorption capacity was found to be 38.3 mg g<sup>-1</sup>. The kinetics of adsorption followed first-order kinetics. The removal efficiency increases with the increase in temperature and hence adsorption process is endothermic in nature. The results of this study forecasts that such magnetic nanoparticle (Fe<sub>3</sub>O<sub>4</sub>) impregnated onto tea waste can very well be recommended for wastewater treatments and control of environmental pollution.

## References

- Z.L. Liu, H.B. Wang, H.Q. Lu, G.H. Du, L. Peng, Y.Q. Du, S.M. Zhang, K.L. Yao, Synthesis and characterization of ultrafine well-dispersed magnetic nanoparticle, *J. Magn. Magn. Mater.* 283 (2004) 258–262.
- J. Hu, G. Chen, M.C. Lo, Selective removal of heavy metals from industrial wastewater using Maghemite nanoparticle: performance and mechanism, *J. Environ. Eng.* 132 (2006) 702–715.
- Y.C. Sharma, V. Srivastava, Separation of Ni(II) ions from aqueous solutions by magnetic nanoparticles, *J. Chem. Eng. Data* 55 (2010) 1441–1442.
- Y.C. Sharma, V. Srivastava, C.H. Weng, S.N. Upadhyay, Removal of Cr (VI) from Wastewater by Adsorption on Iron Nanoparticles, *Can. J. Chem. Eng.* 87 (2009) 921–929.
- Y.C. Chang, D.H. Chen, Adsorption kinetics and thermodynamics of acid dyes on a carboxy methylated chitosan-conjugated magnetic nano-adsorbent, *Macro Mol. Biosci.* 5 (2005) 254–261.
- A.S. Teja, P.Y. Koh, Synthesis, properties, and application of magnetic iron oxide nanoparticles, *Progr Crystal Growth Character Mater.* 55 (2005) 22–45.
- J. Zhou, W. Wu, D. Caruntu, M.H. Yu, A. Martin, J.F. Chen, C.J.O. Connor, W.L. Zhou, Synthesis of porous magnetic hollow silica nanospheres for nanomedicine application, *J. Phys. Chem. C* 111 (2007) 17473–17477.
- V. Padmavathy, P. Vasudevan, S.C. Dhingra, Biosorption of Ni(II) ions on Baker's yeast, *Process Biochem.* (Oxford, UK) 38 (2003) 1389–1395.
- S. Yee Mak, D. Hwang Chen, Binding and sulfonation of poly (acrylic acid) on Iron oxide nanoparticles: a Novel, Magnetic, Strong Acid cation Nano-Adsorbent, *Macromol. Rapid Commun.* 26 (2005) 1567–1571.
- S.Y. Lee, M.T. Harris, Surface modification of magnetic nanoparticles capped by oleic acids: characterization and colloidal stability in polar solvents, *J. Colloid. Interface Sci.* 293 (2006) 401–408.
- P.S. Haddad, T.M. Martins, L.D. Souza-Li, L.M. Li, K. Metze, R.L. Adam, M. Knobel, D. Zanchet, Structural and morphological investigation of magnetic nanoparticles based on iron oxides for biomedical applications, *Mater. Sci. Eng. C* 28 (2008) 489–494.
- D. Hritcu, M.I. Popa, N. Popa, V. Badescu, V. Balan, Preparation and characterization of magnetic chitosan Nanospheres, *Turk. J. Chem.* 33 (2009) 785–796.
- C.R. Krishnamurti, P. Viswanathan, *Toxic Metal in the Indian Environment*, Tata McGraw-Hill Publishing Company Ltd., New Delhi, 1991.
- A. Ewecharoen, P. Thiravetyan, W. Nakbanpote, Comparison of nickel adsorption form electroplating rinse water by coir pith and modified coir pith, *Chem. Eng. J.* 137 (2008) 181–188.
- H. Xu, Y. Liu, J.H. Tay, Effect of pH on Nickel biosorption by Aerobic Granular Sludge, *Bioresour. Technol.* 97 (2006) 359–363.
- K. Kadivelu, K. Thamariselvi, C. Namasivayam, Adsorption of Ni(II) from aqueous solution onto activated carbon prepared from Coirpith, *Sep. Purif. Technol.* 124 (2001) 497–505.
- K. Periyasamy, C. Namasivayam, Removal of Ni(II) from aqueous solution and nickel plating industry wastewater using an agriculture waste: peanut hulls, *Waste Manage.* 15 (1995) 63–68.
- E. Malkoc, Ni(II) removal from aqueous solution using cone biomass of Thuja Orientalis, *J. Hazard. Mater.* 137 (2006) 899–908.
- K.U. Garg, M.P. Kaur, V.K. Garg, D. Sud, Removal of Ni(II) from aqueous solution by adsorption on agriculture waste biomass using a response surface methodological approach, *Bioresour. Technol.* 99 (2008) 1325–1331.
- S. Pacheo, M. Medina, F. Valencia, J. Tapia, Removal of inorganic mercury from polluted water using structured nanoparticles, *J. Environ. Eng. ASCE* 132 (2006) 342–349.
- G.C. Panda, S.K. Das, T.S. Bandopadhyay, A.K. Guha, Adsorption of nickel on Husk of Lathyrus Sativus: behavior and binding mechanism, *Colloids Surf. B Biointerfaces* 57 (2007) 135–142.



- [22] S.S. Tahir, N. Rauf, Thermodynamic studies of Ni(II) adsorption onto bentonite from aqueous solution, *J. Chem. Thermodyn.* 35 (2003) 2003–2009.
- [23] Y.S. Ho, D.A. Jhonwase, C.F. Forster, Batch nickel removal from aqueous solution by Sphagnum moss peat, *Water Res.* 29 (1995) 1327–1332.
- [24] M. Rio, A.V. Parwate, A.G. Bhole, Removal of  $\text{Cr}^{6+}$  and  $\text{Ni}^{2+}$  from aqueous solution using bagasse and fly ash, *Waste Manage.* 22 (2002) 821–830.
- [25] B. Benguella, H. Benaissa, Cadmium removal from aqueous solution by citin: kinetic and equilibrium studies, *Water Res.* 36 (2002) 2463–2474.
- [26] F.N. Acar, E. Malkoc, The removal of chromium (VI) from aqueous solution by *Fagus orientalis* L, *Bioresour. Technol.* 94 (2004) 13–15.
- [27] M. Rafatullah, O. Sulaiman, R. Hashim, A. Ahmad, Adsorption of copper(II), chromium (III), nickel(II) ions from aqueous solution by meranti sawdust, *J. Hazard. Mater.* (2009) 969–977.
- [28] Y. Nuhoglu, E. Malkoc, A. Gurses, N. Canpolat, The removal of Cu(II) from ions from aqueous solutions by *Ulothrix zonata*, *Bioresour. Technol.* 85 (2002) 331–333.
- [29] E. Malkoc, Y. Nuhoglu, The removal of Cr(VI) from synthetic wastewater by *Ulothrix zonata*, *Fresenius Environ. Bull.* 12 (2003) 376–381.
- [30] C.J. Lin, J.E. Chang, Effect of fly ash characteristics on the removal of Cu(II) from aqueous solution, *Chemosphere* 41 (2001) 1185–1192.
- [31] C.W. Cheung, J.F. Porter, G. MacKay, Sorption kinetic analysis for the removal of cadmium ions from effluents using bone char, *Water Res.* 35 (2001) 605–612.
- [32] C.A. Eligwe, N.B. Okolue, C.O. Nwambu, C.I.A. Nwoko, Adsorption, Thermodynamics and kinetics of mercury(II), cadmium(II) and lead(II) on lignite, *Chem. Eng. Technol.* 22 (1999) 45–49.
- [33] P. Panneerselvam, N. Thinakaran, K.V. Thiruvengadaravi, M. Palanichamy, S. Sivanesan, Phosphoric acid modified-Y zeolites: a novel, efficient and versatile ion exchanger, *J. Hazard. Mater.* 30 (2008) 427–434.
- [34] P. Panneerselvam, V. Sathya selva bala, N. Thinakaran, P. Baskaralingam, M. Palanichamy, S. Sivanesan, Removal of Nickel(II) from aqueous solution by adsorption with modified ZSM-5 Zeolites, *Eur. J. Chem.* 6 (2009) 729–736.
- [35] P. Panneerselvam, V. Sathya selva bala, K.V. Thiruvengadaravi, J. Nandagopal, M. Palanichamy, S. Sivanesan, The removal of copper ions aqueous solution using phosphoric acid modified  $\beta$  zeolites, *Ind. J. Sci. Technol.* 2 (2009) 63–66.
- [36] A. Ahamad, M. Rafatullah, O. Sulaiman, M.H. Ibrahim, Y.Y. Chii, B.M. Siddique, Removal of Cu(II) and Pb(II) ions from aqueous solutions by adsorption on sawdust of Meranti wood, *Desalination* 247 (2009) 639–646.
- [37] S. Cay, A. Uyanik, A. Ozasik, Single and binary component adsorption of copper(II) and cadmium(II) from aqueous solutions using tea-industry waste, *Sep. Purif. Technol.* 38 (2004) 273–280.
- [38] M. Malkoc, Y. Nuhoglu, Investigation of Ni(II) removal from aqueous solution using tea factory waste, *J. Hazard. Mater.* 127 (2005) 120–128.
- [39] E. Malkoc, Y. Nuhoglu, Removal of Ni(II) ions from aqueous solutions using waste of tea factory: adsorption on fixed bed column, *J. Hazard. Mater.* B135 (2006) 328–336.
- [40] E. Malkoc, Y. Nuhoglu, Fixed bed studies for the sorption of chromium(VI) onto tea factory waste, *Chem. Eng. Sci.* 61 (2006) 4363–4372.
- [41] P.A. Brown, S.A. Gill, S.J. Allen, Metal removal from waste water using peat, *Water Res.* 16 (2002) 3907–3916.
- [42] T.W. Tee, A.R.M. Khan, Removal of lead, cadmium and zinc by waste tea leaves, *Environ. Technol. Lett.* 9 (1988) 1223–1232.
- [43] G. Sun, X. Xu, Sunflower stalks as adsorbents for color removal from textile wastewater, *Ind. Eng. Chem. Res.* 36 (1997) 808–812.
- [44] S. Laurent, D. Forge, M. Port, A. Roch, C. Robic, L. Vander Elst, R.N. Muller, Magnetic iron oxide nanoparticles: synthesis, stabilization, vectorization, physicochemical characterizations, and biological applications, *Chem. Rev.* 108 (2008) 2064–2110.
- [45] D. Vien, N.B. Colthup, W.G. Fateley, J.C. Grasselli, *The Handbook of Infrared and Raman Characteristic Frequencies of Organic Molecules*, Academic Press, San Diego, USA, 1991.
- [46] A. Kapoor, T. Viraragavan, Heavy metal biosorption sites in *Aspergillus niger*, *Bioresour. Technol.* 61 (1998) 221–227.
- [47] Y.S. Yun, D. Park, J.M. Park, B. Volskey, Biosorption of trivalent chromium on the brown seaweed biomass, *Environ. Sci. Technol.* 35 (2001) 4353–4358.
- [48] R.E. Sievers, J.C. Bailar, Some metal chelates of ethylene diaminetetraacetic acid, diethylene triaminepenta acetic acid, and triethylenetetraamine hexaacetic acid, *Inorg. Chem.* 1 (1962) 174–182.
- [49] L.R. Drake, S. Lin, G.D. Rayson, P.J. Jackson, Chemical modification and metal binding studies of *Datura innoxia*, *Environ. Sci. Technol.* 30 (1996) 110–114.
- [50] S. Lagergren, *Absolute Theory of So-called Adsorption of Soluble Substance*, K. Sven. Vetenskapskad. Handl, 1898.
- [51] K.K. Panday, G.V. Prasad, N. Singh, Copper(II) removal from aqueous solution by fly ash, *Water Res.* 19 (1985) 869.
- [52] I. Langmuir, The constitution and fundamental properties of solids and liquids, Part. I. Solids, *J. Am. Chem. Soc.* 38 (1916) 2221–2295.
- [53] H.M.F. Freundlich, Over the adsorption in solution, *J. Phys. Chem.* 57 (1906) 385–470.
- [54] F.A. Alrub, M. Kandah, N. Aldabaibeh, Nickel removal from aqueous solution by using sheep Manure Waste, *Eng. Life Sci.* 2 (2002) 111–116.
- [55] C. Huang, C. Ying-Chien, L. Ming-Ren, Adsorption of Cu(II) and Ni(II) by palletized biopolymer, *J. Hazard. Mater.* 45 (1996) 265–267.
- [56] A.K. Meena, G.K. Mishra, P.K. Rai, C. Rajgopal, P.N. Nagar, Removal of heavy metal ions from aqueous solution using carbon arogeel as an adsorbent, *J. Hazard. Mater.* 122 (2005) 161–170.
- [57] Z. Reddad, C. Gerente, Y. Andres, M.C. Ralet, J.F. Thibault, P.L. Cloirec, Ni(II) and Cu(II) binding properties of native and modified sugar beet pulp, *Carbohydr. Polym.* 49 (2002) 23–31.
- [58] V. Padmavathy, Biosorption of Ni(II) ions on Baker's yeast: kinetic, thermodynamic and desorption studies, *Bioresour. Technol.* 99 (2008) 3100–3109.
- [59] R. Suemitsu, R. Uenishi, I. Akashi, M. Kakano, The use of dyestuff-treated rice hulls for removal of heavy metals from wastewater, *J. Appl. Polym. Sci.* 31 (1986) 74–83.